Proceedings of the 12th International Conference on the Stability of Ships and Ocean Vehicles, 14-19 June 2015, Glasgow, UK.

A Simplified Simulation Model for a Ship Steering in Regular Waves

Xiechong Gu, *State Key Laboratory of Ocean Engineering*, *Shanghai Jiao Tong University* (*SJTU*), *Shanghai*, *China* xcgu@sjtu.edu.cn

Ning Ma, *State Key Laboratory of Ocean Engineering*, *SJTU*, *China* ningma@sjtu.edu.cn

Jing Xu, *China Ship Development and Design Centre*, *Wuhan*, *China* xujing.sjtu@gmail.com

Dongjian Zhu, *Shanghai Merchant Ship Design and Research Institute* tobya@sjtu.edu.cn

ABSTRACT

A simplified simulation model for a ship steering in regular waves is proposed. It combines the traditional MMG (mathematical manoeuvring group) model with seakeeping model. The former divides hydrodynamic forces into individual ones on the hull, from propeller and due to rudder operation. The latter treats wave forces as the first and second order ones. Impulse response functions, transformed from RAOs, are convoluted with ship motions. Manoeuvring of S175 container ship in regular waves is simulated, and validated by free running tests in regular waves of a S175 model in our ocean engineering basin. Validity and effectiveness of the simulation model are shown.

Keywords: *ship manoeuvring in waves, seakeeping, time domain simulation, impulse response function, second order wave force*

1. INTRODUCTION

Nowadays, manoeuvrability and seakeeping performance has begun to be wholly considered. In the past half a century, manoeuvrability is basically assessed in calm water. A MMG model, out of other theoretical models, was put forward by MMG group in Japan and showed very effective. In MMG model, hydrodynamic forces are split into individual parts, the ones on the ship hull, from the propeller and due to rudder operation, while interactions between them are implicitly, rather than explicitly, shown. Later, Hirano (1981) extended the calm water theory to operation in waves and added second order wave forces into the model. It takes water wave effects into account. Hirano (1981) measured second order wave forces and then calculated turning trajectory in waves. Kijima (1997) further improved the model, taking first order wave forces and roll response into account, and established a 4DOF MMG model. Kijima (1997) investigated effects of waves on turning trajectories. Yasukawa (2008) extended it to 6DOF motion. Accuracy of the simulated turning trajectory of a container ship in regular waves was apparently improved. On the other hand, Skejec (2008) established a unified manoeuvring and seakeeping model, where first order wave loads are evaluated by STF strip theory by Salvesen (1970). Skejec (2008) systematically investigated estimation methods for various hydrodynamic loads, and only those of suitable ones enter into the model. Turning trajectories simulated are much nice.

This paper presents a 6DOF model, of which manoeuvring and seakeeping are integrated. First order and second order wave loads in frequency domain are calculated in terms of

a code by three dimensional panel method. Impulse response functions are derived from the response amplitude operators (RAOs) by Fourier transformation. Motion equations are solved step by step in time domain. Turning trajectories and history of seakeeping motions are simultaneously obtained. For validation, free running tests of a S175 ship model are performed in our ocean engineering basin.

Below, a mathematical model is described at first, where coordinate systems, estimation method for various hydrodynamic loads, motion equations and solution method are shown. Next, numerical results, model ship specifications, simulated and measured turning trajectories and zigzag motions are given. Finally a brief conclusion is stated.

2. MATHEMATICAL MODEL

2.1 General Equations of Motion

Consider a ship travelling in regular waves. As Fig.1 shows, a global coordinate system, $O_0X_0Y_0Z_0$, is established. O_0X_0 coincides with wave propagation direction. Another coordinate system, $Gx_by_bz_b$, is fixed on the ship. G denotes the centre of gravity of the ship. Location G, (x_0, y_0, z_0), in $O_0X_0Y_0Z_0$ and attitude, (φ, θ, ψ), of the ship vary with time t. Heading angle, *i.e.* yaw angle, ψ, is measured from Gx_b to O_0X_0, pitching angle, θ, is from Gx_b to horizontal plane $O_0X_0Y_0$, and roll angle, φ, is from Gz_b to the vertical plane through longitudinal centreline of the ship. We denote (u, v, w) as the velocity at G in $Gx_by_bz_b$, and (p, q, r) as angular velocity of the ship. Relations of Eq.1 and Eq.2 can be derived. In these equations, dot over a symbol, say $\dot{x}_0$, means time derivative of that symbol, say x_0.

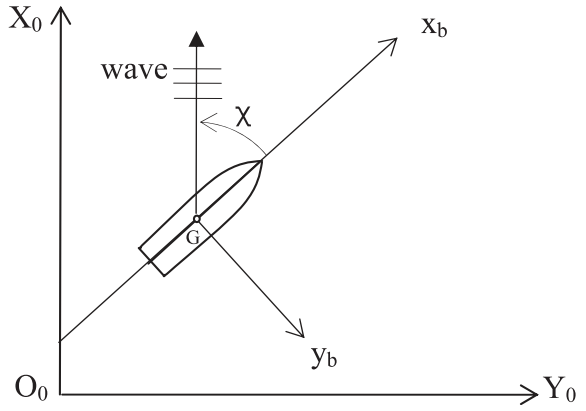

Figure 1 Coordinate Systems

$$\begin{bmatrix}\dot{x}_0\\ \dot{y}_0\\ \dot{z}_0\end{bmatrix}=\begin{bmatrix}\cos\psi\cos\theta & \begin{pmatrix}-\sin\psi\cos\phi+\\ +\cos\psi\sin\theta\sin\phi\end{pmatrix} & \begin{pmatrix}\sin\psi\sin\phi+\\ +\cos\psi\sin\theta\cos\phi\end{pmatrix}\\ \sin\psi\cos\theta & \begin{pmatrix}\cos\psi\cos\phi+\\ +\sin\psi\sin\theta\sin\phi\end{pmatrix} & \begin{pmatrix}-\cos\psi\sin\phi+\\ +\sin\psi\sin\theta\cos\phi\end{pmatrix}\\ -\sin\theta & \cos\theta\sin\phi & \cos\theta\cos\phi\end{bmatrix}\cdot\begin{bmatrix}u\\ v\\ w\end{bmatrix} \tag{1}$$

$$\begin{bmatrix}\dot{\phi}\\ \dot{\theta}\\ \dot{\psi}\end{bmatrix}=\begin{bmatrix}1 & \sin\phi\tan\theta & \cos\phi\tan\theta\\ 0 & \cos\phi & -\sin\phi\\ 0 & \sin\phi/\cos\theta & \cos\phi/\cos\theta\end{bmatrix}\begin{bmatrix}p\\ q\\ r\end{bmatrix} \tag{2}$$

According to MMG model, forces and moments on a ship are written as the sum of those due to ship hull, propeller, rudder where coupling effect between them is not explicitly shown. In addition, components due to wave, both the first order and the second order wave forces, are also added. This results Eq.3, a general equation of ship motions

$$\begin{cases}m(\dot{u}-vr+wq)=X_H+X_P+X_R+X_{1W}+X_{2W}\\ m(\dot{v}+ur-pw)=Y_H+Y_P+Y_R+Y_{1W}+Y_{2W}\\ m(\dot{w}-uq+vp)=Z_H+Z_{1W}\\ I_{xx}\dot{p}=K_H+K_R+K_{1W}\\ I_{yy}\dot{q}+(I_{xx}-I_{zz})pr=M_H+M_{1W}\\ I_{zz}\dot{r}+(I_{yy}-I_{xx})pq=N_H+N_P+N_R+N_{1W}+N_{2W}\end{cases} \tag{3}$$

where subscripts H, P, R, $1W$ and $2W$ stand for the forces or moments due to ship hull, propeller, rudder, the first order and the second order wave forces respectively. m is mass of the ship, and I_{xx}, I_{yy}, I_{zz} are moments of inertia of the ship with respect to axes Gx_b, Gy_b, Gz_b respectively, while other cross components are relatively small and ignored. Whenever general forces on the right hand side of Eq.3 are estimated step by step, motions of the ship are accordingly obtained by solving Eq.3. Estimations of these forces will be given below.

2.2 Propeller Forces

For simplicity, propeller is considered only producing either forward or backward forces,

$$X_P = (1-t_P)\cdot \rho n^2 D_P{}^4 \cdot K_T(J_P) \tag{4}$$

while Y_P and N_P are reasonably neglected. Here ρ is the water density, D_P diameter of the propeller, n rotational speed. Thrust deduction factor t_p is estimated from empirical formulas. $K_T(J_P)$ is open water propeller thrust coefficient, varies with advance coefficient J_P, where wake coefficient is also estimated from an empirical formula.

2.3 Rudder Forces

Rudder forces are dominantly due to the lift force, F_N, on the rudder. It causes mainly drag and drift forces, yawing and heel moments on the ship.

$$\begin{cases} X_R = (1-t_R)F_N \sin\delta \\ Y_R = (1+a_H)F_N \cos\delta \\ N_R = (x_R + a_H x_H)F_N \cos\delta \\ K_R = z_G Y_R \end{cases} \tag{5}$$

where δ is the rudder angle, t_R the rudder drag reduction factor, mainly due to the wake, a_H is drift force modification factor, x_H the distance from rudder centre to G, the centre of gravity of the ship, x_R is the horizontal distance from resultant rudder force to rudder centre, z_G is vertical coordinate of the resultant rudder force.

2.4 Hull Forces

This kind of forces is due to the ship moves advancing in calm water. It can be considered as two parts, one is due to pressures normal to the hull, the other is due to shear stress tangent to the hull.

Eq.6 is the contribution of pressure, which is evaluated by potential flow theory. Eq.7 shows the contribution of shear stress, which could be obtained either from captive model tests or from empirical formulas.

$$\begin{cases} -X_{HI} = A_{11}\dot{u} - A_{22}vr + A_{33}wq \\ -Y_{HI} = A_{22}\dot{v} + A_{11}ur - A_{33}pw \\ -Z_{HI} = A_{33}\dot{w} - A_{11}uq + A_{22}vp \\ -K_{HI} = A_{44}\dot{p} + (A_{66}-A_{55})qr + (A_{33}-A_{22})vw \\ -M_{HI} = A_{55}\dot{q} + (A_{44}-A_{66})pr + (A_{11}-A_{33})uw \\ -N_{HI} = A_{66}\dot{r} + (A_{55}-A_{44})pq + (A_{22}-A_{11})uv \end{cases} \tag{6}$$

$$\begin{cases} X_{HV} = X_{uu}u^2 + X_{vv}v^2 + X_{vr}vr + X_{rr}r^2 \\ Y_{HV} = Y_v v + Y_r r + Y_{|v|v}|v|v + Y_{|r|r}|r|r + Y_{vvr}v^2 r + Y_{vrr}vr^2 \\ Z_{HV} = -Z_w w - Z_q q - Z_{\dot{q}}\dot{q} - Z_\theta \theta \\ K_{HV} = -2K_p p - \rho g \nabla \overline{GM} \sin\varphi - Y_H z_H \\ M_{HV} = -M_w w - M_{\dot{w}}\dot{w} - M_q q - M_\theta \theta \\ N_{HV} = N_v v + N_r r + N_{|v|v}|v|v + N_{|r|r}|r|r + N_{vvr}v^2 r + N_{vrr}vr^2 + Y_H \cdot X_c \end{cases} \tag{7}$$

Subscript I in Eq.6 stands for those due to pressures, and subscript V in Eq.7 for those due to shear stresses, their sum gives the hull forces. For example, X_{HI}+X_{HV} gives out X_H. A_{ij} is the added mass of i-mode motion due to j-mode motion of the ship. ∇ is the volume displaced by the ship, GM the transverse metacentric height of the ship.

2.5 Wave Forces

Wave forces are decomposed into the first order and the second order ones. The former is further separated to the incident wave forces, *i.e.* Froude-Krylov forces, radiation ones and diffraction ones. Panel method is powerful in solution for velocity potential of radiation and diffraction. According to Cummins (1962), the radiation and diffraction forces are expressed as follows.

$$F_{jk}^R = -\mu_{jk}\ddot{\eta}_k(t) - b_{jk}\dot{\eta}_k(t) - c_{jk}\eta_k(t) - \int_0^t K_{jk}(t-\tau)\cdot\eta_k(\tau)d\tau \tag{8}$$

$$F_j(t) = F_j^D + F_j^I = -\int_{-\infty}^{t} H_j(t-\tau)h(\tau)d\tau \tag{9}$$

where superscript R stands for radiation, I and D are for incident wave and diffraction. $h(\tau)$ is the incident wave elevation at the instant τ. $\eta_k(\tau)$

is the moving displacement of mode k motion at the instant τ. The kernel function $K_{jk}(\tau)$ can be obtained from the damping coefficient $B_{jk}(\omega)$

$$K_{jk}(\tau)=\frac{2}{\pi}\int_0^\infty B_{jk}(\omega)\cdot\cos(\omega\tau)d\omega \tag{10}$$

$$\mu_{jk}=A_{jk}^{\infty} \tag{11}$$

$$b_{jk}=B_{jk}^{\infty} \tag{12}$$

that is, μ_{jk} and b_{jk} correspond to the added mass A_{jk} and damping coefficient B_{jk} at extremely high frequency, whereas c_{jk} is restoring forces with nonzero components follows

$$\begin{aligned} c_{33}&=\rho g A_{wp}\\ c_{35}&=c_{53}=-\rho g S_y\\ c_{44}&=\rho g\nabla\overline{GM}_T\\ c_{55}&=\rho g\nabla\overline{GM}_L \end{aligned} \tag{13}$$

where A_{wp} is the water plane area, S_y the first order moment of the water plane with respect to Gy_b axis, GM_T and GM_L are the transverse metacentric height and longitudinal metacentric height respectively.

Kernel function $H_j(t)$ is obtained from the wave force $f_{wj}(\omega)$ due to incident wave of unit amplitude and its corresponding diffraction as follows

$$H_j(t)=\frac{1}{2\pi}\int_{-\infty}^{\infty} f_{wj}(\omega)e^{-i\omega t}d\omega \tag{14}$$

As for the second order drift forces, at first we get the response amplitude operator (RAO) from panel method for different frequencies and heading angles, then at any instant the drift force is evaluated by interpolation of the RAO for the specified encounter frequency and heading angle.

2.6 Numerical Algorithm

In simulation, at first by means of the code based on panel method, radiation and diffraction problems are solved, then added mass and damping coefficient are evaluated, and kernel functions $K_{jk}(\tau)$ and $H_j(t)$ are calculated. At last, the 4th order Runge-Kutta method is applied to solve Eq.3 in time domain step by step.

3. NUMERICAL RESULTS

3.1 Ship for simulation

In simulation, the S175 container ship is used. Table 1 lists principal particulars of S175. Fig.2 shows meshes. In total 1968 quadrilateral meshes are used in calculation.

At first, linear wave force, added mass and damping coefficients, motion response and the second order wave force are calculated by the

Table 1. Principle particulars of S175

symbol	magnitude	unit
L_{OA}	183.0	m
L_{PP}	175.0	m
L_{WL}	178.2	m
B	25.4	m
D	15.0	m
d	9.5	m
∇	24380.6	m^3
C_B	0.5774	
KM	10.5	m
x_B (from AP)	80.64	m
k_{xx}	8.5852	m

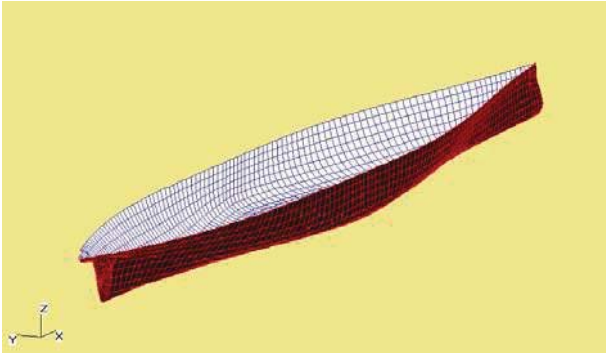

Figure 2 Meshes of S175 for Simulation

using the code based on panel method. In calculation, encounter wave frequency is in between 0.1 and 12 *rad/s*, with increment 0.1 *rad/s*. Heading angle relative to the wave is in between 0 to 360 *deg*, with increment 10 *deg*. It is found that results for 1968 meshes show almost no significant difference with those for more meshes, say 3156 meshes. Service speed corresponds Froude number 0.166. The second order wave force for specified encounter wave frequency and heading angle is evaluated from the computed results by applying Lagrange interpolation algorithm.

Fig.3 to 8 show response amplitude operators (RAOs) of motions. Fig.9 and 10 are the calculated added mass and damping coefficient. Fig.11 shows the first order wave forces and moments in beam waves. Fig.12 shows the second order wave forces and moments in beam waves.

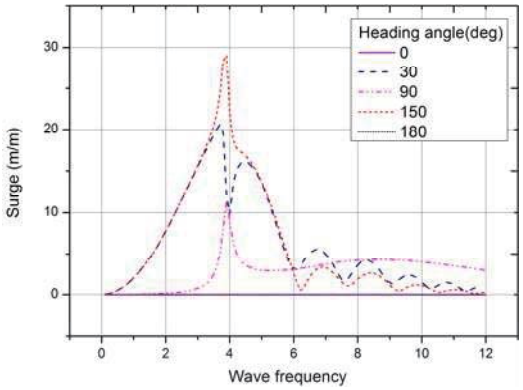

Figure 3 RAO of Surge

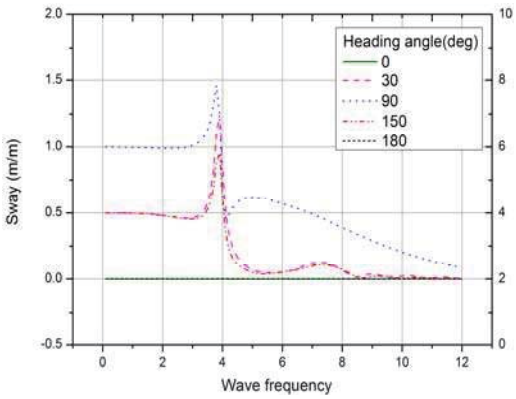

Figure 4 RAO of Sway

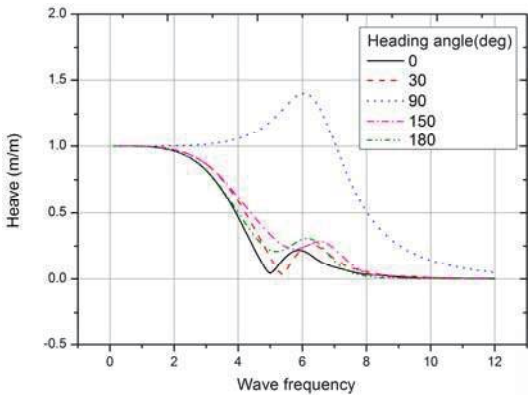

Figure 5 RAO of Heave

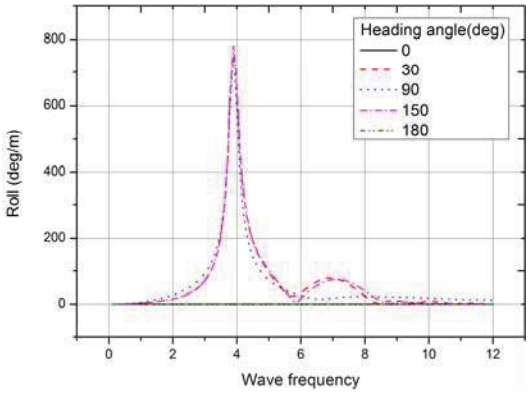

Figure 6 RAO of Roll

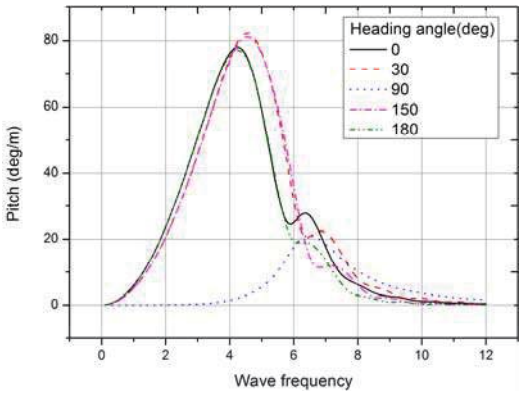

Figure 7 RAO of Pitch

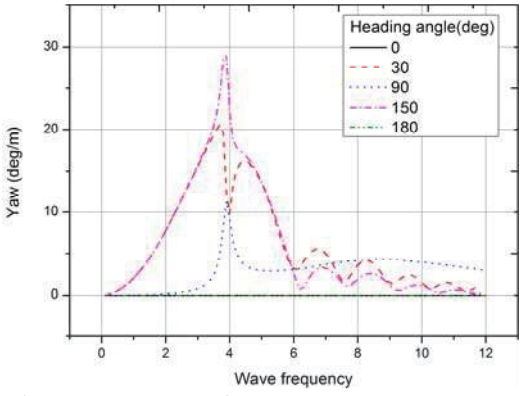

Figure 8 RAO of Yaw

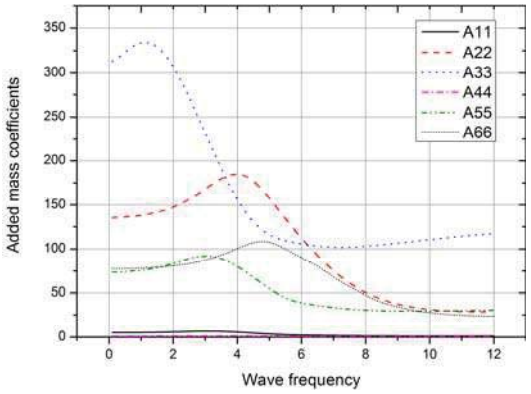

Figure 9 Added Mass

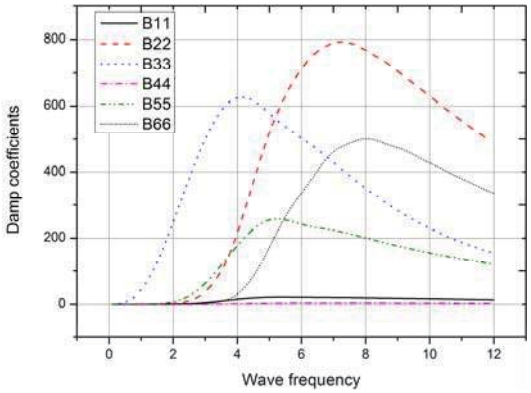

Figure 10 Damping Coefficient

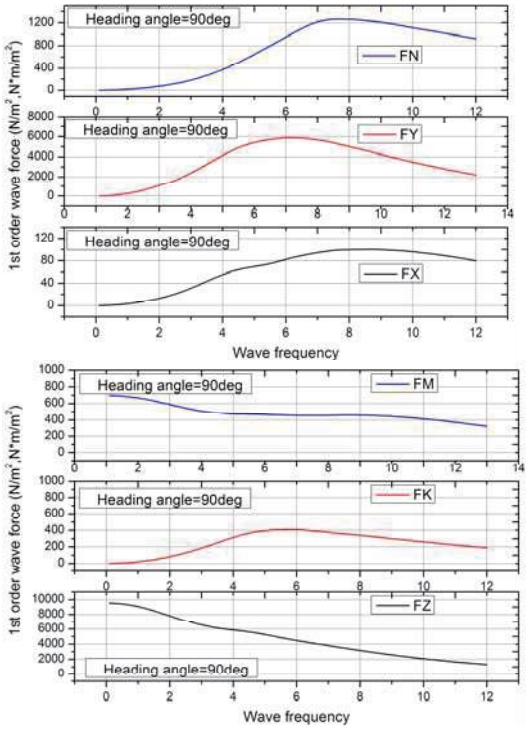

Figure 11 The First Order Wave Forces in Beam Waves

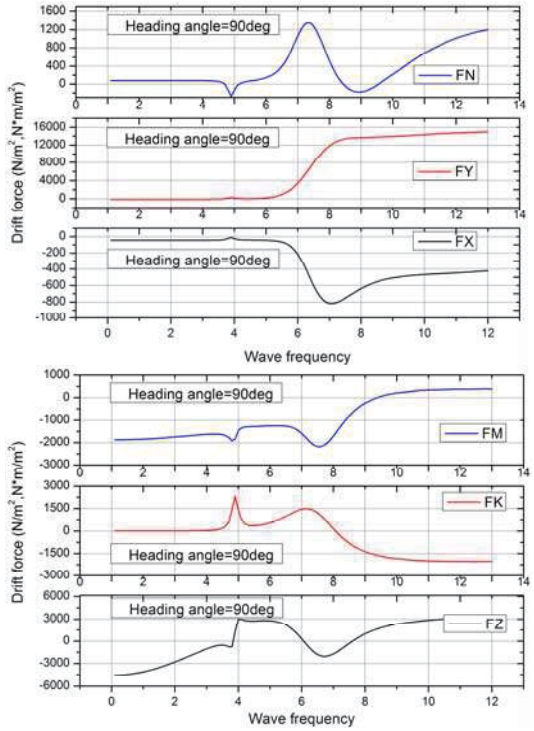

Figure 12 The Second Order Wave Forces in Beam Waves

Figure 13 Ship Model of S175

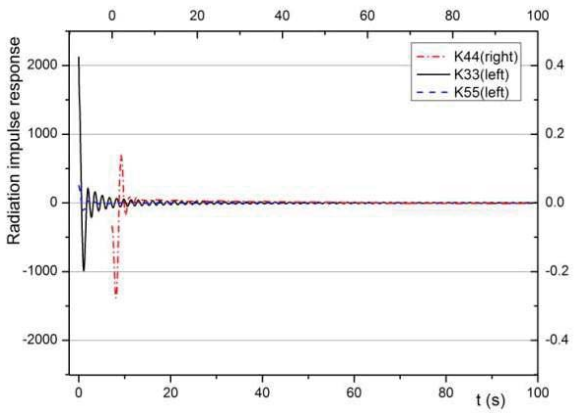

Figure 14 Radiation Impulse Responses

Equations of motion to be solved are summarized in Eq.15. In order to validate simulation method, a free running test for a S175 ship model, see Fig.13, with scale factor 57.69 was performed in the ocean engineering basin of Shanghai Jiao Tong University. Fig.14 shows the calculated radiation impulse responses.

$$
\begin{cases}
m(\dot{u}-vr+wq)+A_{11}\dot{u}-A_{22}vr+A_{33}wq+\int_0^t K_{11}(t-\tau)\cdot u d\tau+\int_{-\infty}^t H_{11}(t-\tau)\cdot h(\tau)d\tau \\
\quad = X_{HV}+X_P+X_R \\
m(\dot{v}+ur-pw)+A_{22}\dot{v}+A_{11}ur-A_{33}pw+\int_0^t K_{22}(t-\tau)\cdot v d\tau+\int_0^t K_{24}(t-\tau)\cdot p d\tau \\
\quad +\int_0^t K_{26}(t-\tau)\cdot r d\tau+\int_{-\infty}^t H_{22}(t-\tau)\cdot h(\tau)d\tau = Y_{HV}+Y_P+Y_R \\
m(\dot{w}-uq+vp)+A_{33}\dot{w}-A_{11}uq+A_{22}vp+C_{33}\cdot\eta_3(t)+C_{35}\cdot\eta_5(t)+B_{33}w+B_{35}q \\
\quad +\int_0^t K_{33}(t-\tau)\cdot w d\tau+\int_0^t K_{35}(t-\tau)\cdot q d\tau+\int_{-\infty}^t H_{33}(t-\tau)\cdot h(\tau)d\tau = Z_{HV} \\
I_{xx}\dot{p}+A_{44}\dot{p}+(A_{66}-A_{55})qr+(A_{33}-A_{22})vw+B_{44}\cdot p+C_{44}\cdot\eta_4(t)+\int_0^t K_{44}(t-\tau)\cdot p d\tau \\
\quad +\int_0^t K_{42}(t-\tau)\cdot v d\tau+\int_0^t K_{46}(t-\tau)\cdot r d\tau+\int_{-\infty}^t H_{44}(t-\tau)\cdot h(\tau)d\tau = K_{HV}+K_R \\
I_{yy}\dot{q}+(I_{xx}-I_{zz})pr+A_{55}\dot{q}+(A_{44}-A_{66})pr+(A_{11}-A_{33})uw+C_{55}\cdot\eta_5(t)+C_{53}\eta_3(t) \\
\quad +B_{53}\cdot w+B_{55}\cdot q+\int_0^t K_{55}(t-\tau)\cdot q d\tau+\int_0^t K_{53}(t-\tau)\cdot w d\tau+\int_{-\infty}^t H_{55}(t-\tau)\cdot h(\tau)d\tau = M_{HV} \\
I_{zz}\dot{r}+(I_{yy}-I_{xx})pq+A_{66}\dot{r}+(A_{55}-A_{44})pq+(A_{22}-A_{11})uv+\int_0^t K_{66}(t-\tau)\cdot r d\tau \\
\quad +\int_0^t K_{62}(t-\tau)\cdot v d\tau+\int_0^t K_{64}(t-\tau)\cdot p d\tau+\int_{-\infty}^t H_{66}(t-\tau)\cdot h(\tau)d\tau = N_{HV}+N_P+N_R-Y_{HV}\cdot x_c
\end{cases}
\tag{15}
$$

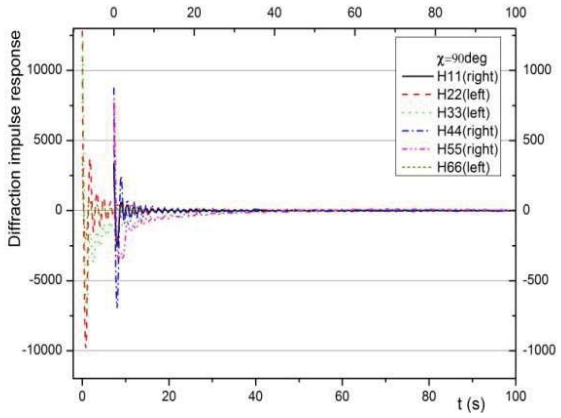

Figure 15 Diffraction Impulse Responses

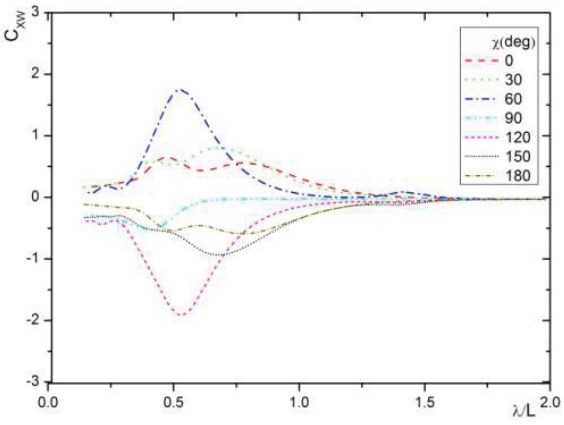

Figure 16 Longitudinal Second Order Wave Force Coefficients

Fig.15 gives out the calculated diffraction impulse responses at beam waves. Fig.16, 17 and 18 show the calculated results of longitudinal, lateral and yawing second order wave forces at various heading angles.

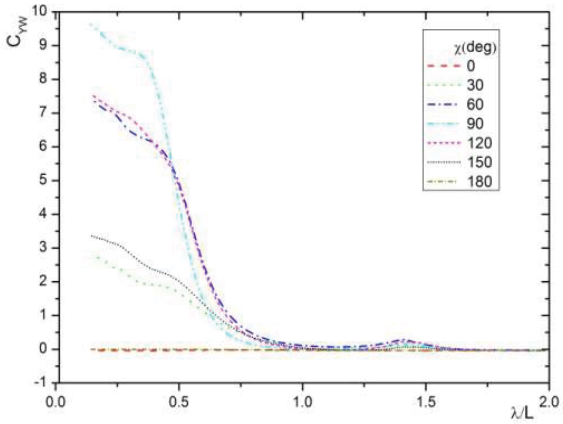

Figure 17 Lateral Second Order Wave Force Coefficients

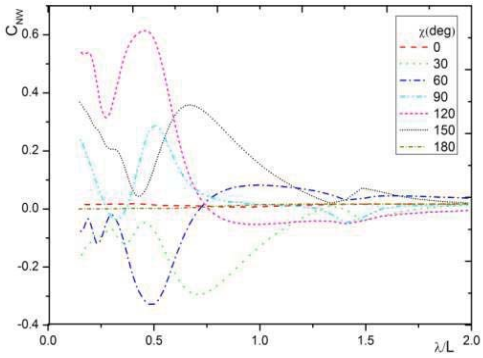

Figure 18 Yawing Second Order Wave Moment Coefficients

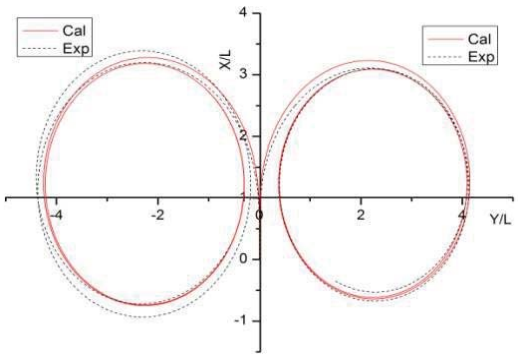

Figure 19 Turning Circle in Still Water with Rudder Angle ±35°

Based on the above results, turning circle and zigzag test are simulated by solving Eq.15 numerically. Fig.19 shows that in still water the simulated circles agree quite well to measured ones at rudder angles of left and right 35° . Fig.20 and 21 demonstrates that in still water the simulated zigzag results are very close to the measured records.

Now wave is introduced. As above, initial speed of the ship model is unchanged, also 0.72 *m/s*. Fig.22 is a comparison of the simulated turning circle in head wave with the test record.

Amplitude of the wave is 13.5 *mm*, and the ratio of wavelength to ship model length is 1.4. It can be seen that the turning circle drifts along the wave propagating direction downwards. The second order wave drift force seems the main cause of this phenomenon. Agreement of the simulated one with the test result is still quite good.

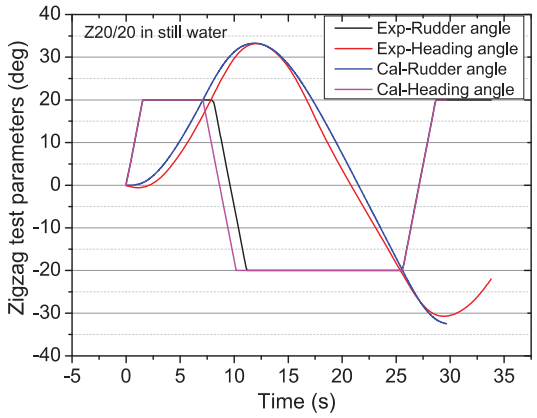

Figure 20 20/20° Zigzag in Still Water

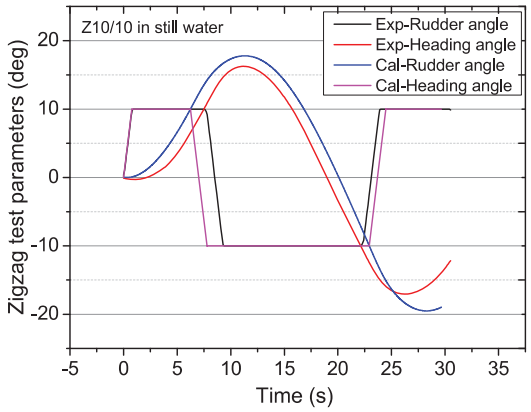

Figure 21 10/10° Zigzag in Still Water

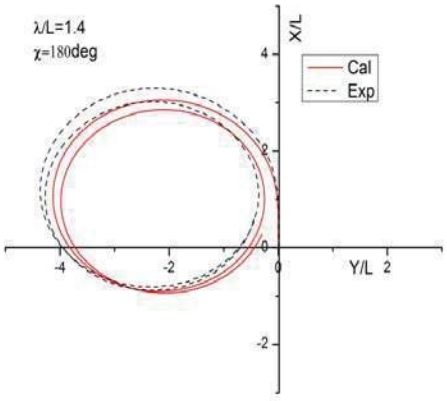

Figure 22 Turning Circle in a Head Wave

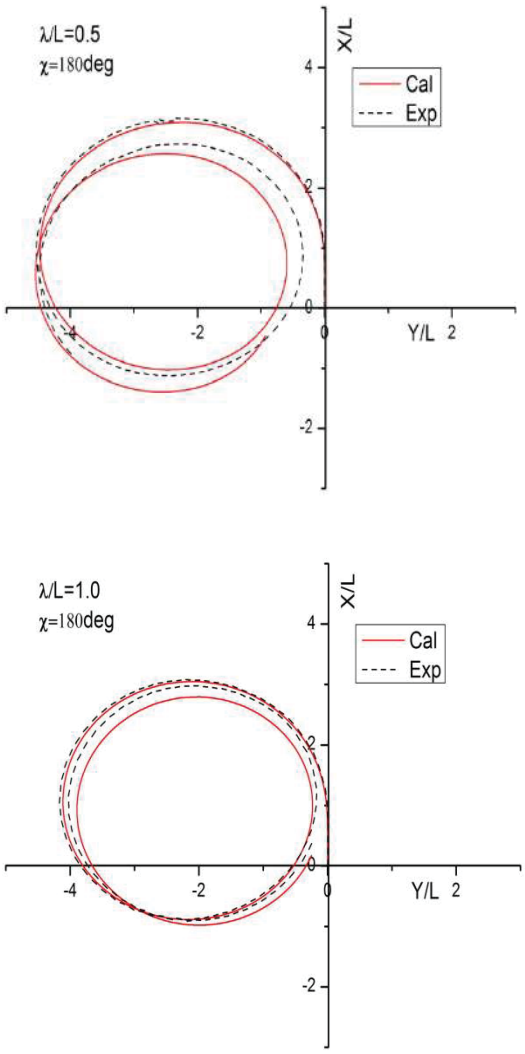

Figure 23 Turning Circle in Head Waves with Different Wave Lengths

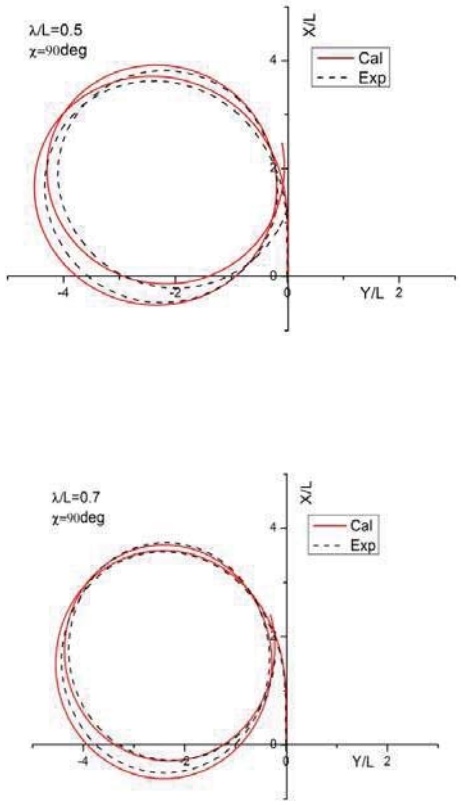

Figure 24 Turning Circle in Beam Waves with Different Wave Lengths

Fig.23 and 24 show turning circles in head and beam waves with different wavelengths. Agreement of the simulated ones with the test results is also quite good.

4. CONCLUSION

A simplified simulation method for a ship steering in regular waves is developed. The traditional MMG (mathematical manoeuvring group) model is combined with the Cummins seakeeping model. The former separates hydrodynamic forces into several individual parts due to different causes, such as the ones on the ship hull, from propeller and due to rudder operation. The latter takes linear and second order wave forces into account.

Based on the investigation for S175 ship, this method seems valid and effective enough. Since a ship steering in waves is affected by a lot of factors, and their mechanisms are quite specific and complicated, further systematic investigations is needed and will be done later, especially for validation, model tests in steeper waves is urgent.

5. ACKNOWLEDMENTS

This study is a part of Project 51279105 which is financially supported by the National Foundation of China.

6. REFERENCES

Cummins W.E., 1962, “The Impulse Response Function and Ship Motions”, Schiffstechnik 9, pp. 101-109

Hirano, M., Takashima, J., Takeshi, K. and Saruta T., 1981, “Ship turning trajectory in regular waves”, West Japan Society of Naval Architects, Vol. 60, pp. 17-31

Kijima, K., Furukawa, Y., 1997, “Ship maneuvering performance in waves”, Proceedings of 3rd International Stability Workshop

Salvesen, N., Tuck, E. 0. and Faltinsen, 0., 1970, “Ship Motions and Ship Loads”, Trans. SNAME, Vol. 78, pp. 250-287

Skejec, R. and Faltinsen, O.M., 2008, “A Unified Seakeeping and Maneuvering Analysis of Ships in Regular Waves”, Journal of Marine Science Technology, Vol. 13, No. 4, pp. 371-394

Yasukawa, H., 2008, “Simulations of Ship Maneuvering in Waves”, Journal of the Japan Society of Naval Architects and Ocean Engineers, Vol. 7, pp. 163-170